Translational Stroke Research (2018) 9:437–451
https://doi.org/10.1007/s12975-017-0593-8

REVIEW

Photothrombotic Stroke as a Model of Ischemic Stroke

Anatoly B. Uzdensky[1]

Received: 18 August 2017 / Revised: 14 November 2017 / Accepted: 24 November 2017 / Published online: 29 November 2017

Abstract
The search of effective anti-stroke neuroprotectors requires various stroke models adequate for different aspects of the ischemic processes. The photothrombotic stroke model is particularly suitable for the study of cellular and molecular mechanisms underlying neurodegeneration, neuroprotection, and neuroregeneration. It is a model of occlusion of small cerebral vessels, which provides detailed study of molecular mechanisms of ischemic cell death and useful for search of potential anti-stroke agents. Its advantages include well-defined location and size of ischemic lesion that are determined by the aiming of the laser beam at the predetermined brain region; easy impact dosing by changing light intensity and duration; low invasiveness and minimal surgical intervention without craniotomy and mechanical manipulations with blood vessel, which carry the risk of brain trauma; low animal mortality and prolonged sensorimotor impairment that provide long-term study of stroke consequences including behavior impairment and recovery; independence on genetic variations of blood pressure and vascular architecture; and high reproducibility. This review describes the current application of the photothrombotic stroke model for the study of cellular and molecular mechanisms of stroke development and ischemic penumbra formation, as well as for the search of anti-stroke drugs.

Keywords Photothrombotic stroke · Ischemia · Penumbra · Neurodegeneration · Neuroprotection

Ischemic Stroke and Neuroprotection Problem

Ischemic stroke is one of the major factors of human disability and death. It is responsible for more than 5.5 million human deaths each year worldwide [1]. Blockage of blood vessels very rapidly, for few minutes, leads to oxygen and glucose deficit, ATP depletion, generation of reactive oxygen species (ROS), oxidative stress, injury of cellular membranes, loss of ionic gradients, depolarization, excitotoxicity, edema, necrosis, and brain tissue infarct [2, 3]. In such short time, it is practically impossible not only to treat, but even to diagnose stroke.

The damaging processes propagate from the infarction core to the surrounding tissue. Tissue lesion in the peri-infarct zone (or zone at risk or ischemic penumbra) develops slower, for several hours, and this "therapeutic window" provides time for cell protection. The concept that ischemic penumbra (or shorter - penumbra) is potentially salvageable is the basis of numerous searches of neuroprotective medications, which can save the penumbra tissue and limit negative stroke consequences [4]. More than 1000 preclinical studies and more than 200 clinical trials were performed. However, no one drug with proven neuroprotective efficiency and without harmful adverse side effects has been found yet. Even medications that protected ischemic cell cultures and experimental animals were not efficient in humans or caused harmful adverse effects [1, 5–11]. Therefore, the comprehensive studies of the molecular basis of neurodegeneration and neuroprotection in penumbra are needed for development of novel approaches for treatment of stroke consequences [12, 13]. Adequate stroke models that represent different aspects of stroke development are necessary [1, 14, 15].

Animal Models of Stroke

Human ischemic stroke (about 80% of all stroke cases) is caused either by large vessel atherosclerosis and rupture of artherosclerotic plaques (about 50% of cases), or by

✉ Anatoly B. Uzdensky
auzd@yandex.ru

[1] Laboratory of Molecular Neurobiology, Academy of Biology and Biotechnology, Southern Federal University, 194/1 Stachky prospect, Rostov-on-Don 344090, Russia

cardioembolism (20%), or by small vessel injury (lacunar infarct of subcortical white matter, about 25%) [15]. A number of animal models of cerebral ischemia are currently used for the study of cellular and molecular mechanisms of ischemic brain damage and for testing of new anti-stroke neuroprotectors [1, 14–19]. Different rodent stroke models display various but not all aspects of human stroke.

Acute global ischemia is commonly induced either by permanent ligation of both vertebrate arteries and temporary ligation of two common carotid arteries (four-vessel occlusion model), or only by temporary ligation of two common carotid arteries (two-vessel occlusion model). These methods result in extensive, but reversible bilateral lesion of forebrain, mainly white matter. They are relevant to cardiac arrest and asphyxia in humans. Their disadvantages include complicated surgery, occurrence of seizures, variable outcome and poor reproducibility. Global ischemic models are less relevant to human stroke than the focal stroke models.

Focal models of ischemic stroke are more realistic for human stroke. They are more complicated than global ischemia because of temporal and spatial heterogeneity. Focal ischemic stroke is usually the result of permanent or transient occlusion of the middle cerebral artery (MCAO). In the permanent model, long-lasting arterial blockade is created, for example, by electrocoagulation of vessels or by intra-arterial insertion of a silicon-coated nylon thread for one or more days. In transient focal ischemia models, the bloodstream is usually blocked mechanically by the nylon filament for 0.5–2 h. This method provides well reproducible infarct size and does not require craniotomy. Timing of occlusion determines the extent and location of ischemic lesion. The MCAO model is characterized by the large infarct volume. It exhibits an ischemic penumbra similar to that of human stroke and is well reproducible. The reperfusion and duration of ischemia are quite controllable. This procedure is relatively easy and not time-consuming. The MCAO model has been used in many studies of molecular mechanisms of ischemic stroke, neurodegeneration, cerebral inflammation, and damage of blood–brain barrier [14–19]. However, MCAO requires anesthesia and significant surgical skill. It is characterized with a risk of vessel rupture, hemorrhage, and high mortality due to large infarct. It often induces hypothalamus damage that rarely occurs in human stroke [19]. The transient ischemia is followed by prompt tissue reperfusion that causes secondary oxidative tissue injury. In the case of permanent ischemia, no reperfusion occurs. The mechanical occlusion models poorly reflect the hemodynamic aspects of thrombolytic reperfusion and not suitable for thrombolysis studies [14–19].

The most common ischemic damage in humans encompasses 4–14% of the brain hemisphere tissue. In these cases, the neuroprotective therapy can be applied. More than 39% ischemic brain damage is classified as a malignant brain infarction with minimal possibility of functional recovery and high mortality [19, 20]. MCAO-induced ischemic stroke in rodents damages commonly 21–45% of the ipsilateral hemisphere. Therefore, the MCAO model reproduces malignant rather than common human stroke. It should be noted that rodents can survive and recover brain functions after stronger brain damage than humans [21].

The thromboembolic model of focal cerebral ischemia is similar to the transient focal ischemic model, but arteries are occluded by the exogenous thrombin clot, or synthetic macrospheres (300–400 μm) or microspheres (< 50 μm) injected into internal carotid artery. This method is relevant to human stroke, but location, size, and duration of ischemia are difficult to control and reproduce. It also requires anesthesia. Nevertheless, these experimental models provide a lot of information on the stroke pathophysiology [15–19].

In 1985, Watson and coworkers have suggested another model of ischemic stroke — photothrombotic stroke, in which focal infarct of the animal cerebral cortex is induced by localized photodynamic effect. Under light exposure, the hydrophilic dye such as Rose Bengal (RB) or erythrosine B, which poorly penetrates cells and remains in the brain vasculature, induces localized oxidative lesion of endothelial membranes, platelet aggregation, and occlusion of microvessels followed by cerebral blood flow (CBF) interruption [22].

Photodynamic Effect and Photodynamic Therapy

Photodynamic therapy (PDT) effect is killing of stained cells under light exposure in the presence of oxygen. After light absorption, the energy of photoexcitation is transferred from the photosensitizing dye molecules to oxygen and turns it into highly reactive singlet form and other ROS. Following oxidative stress induces cell death. The photosensitizing dye (PS), light, and oxygen are non-toxic individually, but their combination damages cells [23–25]. PDT is currently used for killing of malignant cells and treatment of various cancer forms [26, 27] including brain cancer [28, 29]. PS accumulates in tumors, where its level 3–30 times higher than in surrounding healthy tissues. This provides selective, local, and contactless tumor destruction with minimal toxicity to surrounding healthy tissue, absence of long-term side effects, the possibility of multiple repetition and combination with other treatment modalities, and short treatment duration. The optimal properties of PS include high absorption of red light in the "therapeutic window" (600–800 nm), where photons penetrate deeper into the tissue, high quantum yield of singlet oxygen, selective accumulation in tumors, rapid elimination after the treatment, non-toxicity, and low price. Various dye classes such as porphyrins, chlorines, phthalocyanines, and others are used in PDT [26, 30].

The main stages of PDT include PS delivery and selective staining of a tumor, light exposure, cell killing, tumor destruction, removal of destroyed cells, and wound healing. The

pharmacokinetics of PS depends on its hydrophobicity/hydrophilicity and intra-molecular distribution of polar groups. Hydrophobic PSs are located in the lipid bilayer inside the plasma membrane and membranes of intracellular organelles. However, in the bloodstream they aggregate and precipitate. Hydrophilic PS cannot cross the cell membrane. They may penetrate the cell by means of pinocytosis after adsorption on the cell surface. After intravenous administration, the major fraction of hydrophilic PSs remains in blood vessels [31–33].

Here we concentrate on the non-oncological application of PDT—its ability to induce focal photothrombotic brain infarct. In this case, hydrophilic PSs that poorly penetrate cells and remain in the brain vasculature are used.

Photothrombotic Stroke as a Model of Ischemic Stroke

In the photothrombotic stroke (PTS) model, the focal cerebral infarct is induced by photodynamic effect of anionic xanthene dyes such as Rose Bengal (RB) or erythrosine B. After injection, these water-soluble PSs do not cross the blood-brain barrier (BBB) and remain in the bloodstream, where they bind to the vascular endothelium, platelets and other blood cells. Upon localized laser irradiation, these PSs efficiently generate singlet oxygen, which causes oxidative damage to membranes in the vascular endothelium, platelet aggregation, and occlusion of small vessels that leads to ischemia and death of brain cells [22, 34, 35]. Rose Bengal or erythrosine B (15–25 mg/kg) are administrated intraperitoneally (in mice) or intravenously (in rats). In these small rodents laser radiation easy passes through the thin cranial bone. The scattered light is eventually absorbed by PS molecules after multiple scatterings. The wide absorption band of RB (480–560 nm in water or 500–580 nm in the presence of a protein that mimics a cell) has a maximum near 550 or 560 nm and a shoulder at 510–520 or 520–540 nm, respectively [36]. Different light sources that emit light in this spectral region have been used for PTS induction: collimated and filtered white light (560 nm) [22], krypton laser (568 nm) [18], dye laser (562 nm) [37], or laser diode (532 nm) [38–41]. Although the 532 nm wavelength does not fit the absorption maximum, light absorption in the spectral shoulder is sufficient for inducing of localized cerebral infarct. Since light scattering in white matter more than four times higher as compared with gray matter, the low-intense light exposure may induce photothrombosis predominately in white matter [42]. Good practical guidance for PTS techniques have been recently published [42–44].

Photothrombotic stroke is the unique model of occlusion of small cerebral vessels. Unlike occlusion of only one artery that occurs usually in human stroke, PTS impairs the blood flow in a number of superficial vessels within the area exposed to light. In comparison with other stroke models, its advantages include the predictable and well-defined location of an ischemic lesion that is determined by the aiming of the laser beam at the predetermined brain region, the degree of ischemic lesion is determined by light intensity and duration and may be easily managed, the lesion is well reproducible due to the stereotaxic accuracy of irradiation and continuous monitoring of light intensity, simplicity of execution, low invasiveness and minimal surgical intervention, low animal mortality (< 10%), prolonged sensorimotor impairment that provides long-term study of stroke consequences and behavior impairment and recovery, and independence on genetic variations of blood pressure and vascular architecture. PTS does not require craniotomy and mechanical manipulations with blood vessel such as ligation or filament insertion, which carry the risk of local brain trauma. The molecular mechanism of neurodegeneration in PTS is in general similar to that in focal human stroke. This is a model of permanent ischemia. Unlike MCAO that produces ischemic lesion without the participation of platelet aggregation, which primarily promotes brain ischemia in humans, platelet aggregation plays the important role in PTS-induced vessel occlusion. So, this model can be used for the study of the thrombosis-associated inflammation and apoptosis [45].

However, PTS does not mimic well all aspects of acute human stroke. PTS simultaneously induces cytotoxic (intracellular) and vasogenic (extracellular) edema with rapid breakdown of the blood-brain barrier [15, 19, 45–47]; whereas, acute human stroke is characterized by a primary cytotoxic edema, followed by vasogenic edema in several hours [15, 19, 45]. Another disadvantage of PTS as compared with other focal stroke models is rather narrow or absent of the salvageable ischemic penumbra due to intense development of tissue necrosis and edema. A little or no local collateral blood flow and reperfusion are observed in this area [45]. Since the ischemic penumbra, or "tissue at-risk," is the major target of neuroprotective therapy, the translational impact of this model seems to be limited [15].

Recently, the technique of photothrombotic occlusion of the middle cerebral artery (MCAO-PTS) in mice has been developed [48, 49]. In this method, the temporalis muscle was carefully resected from the temporal bone. Then the bone was thinned using the dental burr till it became so transparent that the MCA was visible. After RB administration, a laser beam was directed to MCA through the lens or optical fiber. MCAO-PTS is well reproducible: the coefficient of variation of the lesions was 22–28% as compared with 70% in the traditional MCAO stroke model [48]. Histopathological study showed slightly shrunk nuclei and swollen neuropil at 1 h after MCAO-PTS in rats; nuclear pyknosis, cytoplasmic eosinophilia, vacuolization, and vasogenic edema at 3 h; severe pyknosis and extensive cytotoxic and vasogenic edema at 6–12 h; extensive neuron necrosis with structural disintegration

and peripheral inflammatory infiltration at 1–9 days. Magnetic resonance imaging confirmed this data [46]. Unlike MCAO, MCAO-PTS better reproduces the pathophysiology of thrombosis in clinic, in which platelet aggregates occlude MCA. Using laser speckle contrast imaging (LSCI), in which coherent light (660 nm) incident to a surface produces a reflected speckle pattern that depends on movements of the underlying light-scattering particles such as red blood cells, and recently developed multi exposure speckle imaging techniques, it was shown that MCAO-PTS almost completely suppressed CBF in the irradiated region of the mouse cerebral cortex [50].

Several stages of photothrombotic occlusion of main and branch cortical vessels with different vascular mechanics and hemodynamics were characterized with high spatial and temporal resolution using a microscopic LSCI system [51]. The combination of RB-PTS and confocal optical imaging provided a time-lapsed observation of clot formation dynamics in a single cortex vessel and assessed cellular responses within the mouse CNS in vivo [44]. Using a stereotaxically implanted optic fiber, photothrombotic infarct was induced in the rat caudoputamen [52], or in the internal capsule of the rat brain. The resulting white matter infarction caused a significant motor deficit [43, 53].

The accurate location of the PTS-induced damage allows studying the behavioral deficit associated with the injured area in the cerebral cortex. Stroke-induced sensorimotor dysfunction and following function restoration in stroke patients are associated with the reorganization of peri-infarct area and the similar area in the contralateral hemisphere [54]. Using PTS model, one can identify molecular and cellular events that lead to the reorganization and restoration of brain functions due to neuronal plasticity [55]. The two-dimensional real-time monitoring of PTS-induced CBF impairments in conscious and freely moving rats was performed with a high spatiotemporal resolution using the LSCI technology [56]. Similarly, the dynamics of motor deficit and recovery after PTS were studied with high temporal and spatial resolution in freely running mice. This method, which does not use anesthetics, was proposed as an optimal model for neurobehavioral evaluation in the preclinical anti-stroke drug screening [57]. PTS was also used in studies of the mechanisms of neuroregeneration in rodents. A localized PTS in the mouse motor cortex stimulated axon sprouting within the spinal cord areas that were innervated previously by the injured cortex region. This is an example of neural plasticity associated with functional recovery [58]. Harrison et al. (2013) studied the post-stroke functional reorganization in the sensorimotor cortex of transgenic mice that expressed light-sensitive channelrhodopsin-2. Using noninvasive motion sensors, the authors recorded evoked motor activity in cortical neurons. Targeting of light pulses to an array of cortical points, they obtained a map of the forelimb somatosensory cortex. PTS decreased the motor output in the infarct area and induced the spatial displacement of the sensory and motor maps. Therefore, surviving cortical regions show which functions have been performed by the stroke-damaged areas [59].

PTS mimics the ischemic occlusion of small cerebral vessels, which leads to cerebral microinfarct. As noted by Talley Watts et al., PTS-induced focal microinfarct is clinically relevant to "silent" stroke that can lead to non-lethal, subclinical impairment of cognitive functions such as decline in memory, decision-making, and behavior changes. Patients with silent stroke are often unaware they have suffered a stroke; but over time, multiple silent strokes lead to considerable cognitive impairments.

Human stroke is commonly the result of acute occlusion of major brain arteries such as middle cerebral artery. Significant symptoms of stroke such as paralysis, sensory loss and difficult speaking that occur after MCAO or transient ischemic attack are not observed after PTS [44]. Nevertheless, the neurodegeneration and neuroprotection processes in PTS-induced cerebral microinfarct have the same nature as in classical stroke. Using PTS model, one can better understand stroke pathophysiology and explore new neuroprotective approaches for stroke treatment.

Mechanisms of PTS-Induced Brain Injury

Pathological processes in the PTS core (Fig. 1) include several interlinked components similar to that in human stroke and other stroke models, but have some specific features. The classical PTS model is characterized with rapid progression of ischemic cell death. Photodynamic generation of singlet oxygen and free radicals is believed to induce platelet activation and thrombus (or thrombi) formation. Subsequent occlusion of small vessels reduces delivery of glucose and oxygen that suppresses oxidative phosphorylation and ATP production. Following activation of anaerobic glycolysis increases production of lactic acid and causes tissue acidosis. ATP loss leads to failure of Na^+/K^+-ATPase, fall of ionic gradients, and Na^+ influx and efflux of K^+ in neuronal and glial cells [60, 61]. Extracellular K^+ induces widespread anoxic depolarization in neighboring neurons and glia [62]. Cytosolic Ca^{2+} and oxidative stress play the pivotal role in ischemic cell damage. Ca^{2+} can penetrate through the ionotropic glutamate receptors in the plasma membrane, and release into cytosol from the intracellular stores: the mitochondria and endoplasmic reticulum (ER). Massive glutamate release from injured neurons activates NMDA and AMPA channels in the depolarized neighboring neurons, through which numerous Ca^{2+} ions enter these cells. This further boosts the initial ischemic insult and promotes injury propagation and formation of the penumbra [63]. Ca^{2+} activates calpain and endonucleases, which cleave DNA to cause apoptosis. Calpain hydrolyzes various cellular proteins, ruptures lysosomes, and releases cathepsins. The uncontrolled proteolysis mediated by calpain and cathepsins in

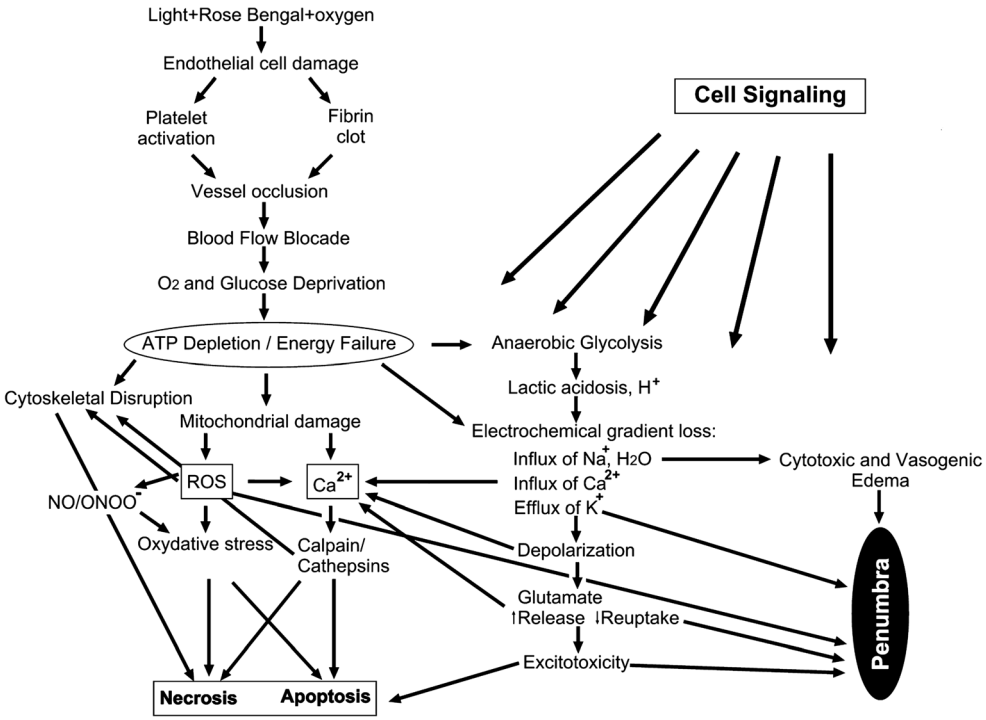

Fig. 1 The scheme of the stroke-induced processes and penumbra formation

neurons and glial cells contribute to neurodegeneration [64]. Ca^{2+} accumulation in mitochondria by Ca^{2+} uniporter decreases mitochondrial potential [65]. The perturbation of electron transport causes leakage of electrons that react with oxygen to produce superoxide-anion (O_2^-) [66] that is followed by formation of hydrogen peroxide (H_2O_2) and hydroxyl radical ($OH^•$). Ca^{2+}-activated neuronal NO synthase produces nitric oxide that turns into peroxynitrite ($ONOO^-$) by reacting with O_2^- [67, 68]. ROS-induced oxidative stress is the major cause of tissue lesion [69]. ROS also stimulate some signaling proteins and transcription factors that regulate cell survival and death such as MAP kinases p38 and JNK, NF-κB, and AP-1 [70]. Oxidative damage of ER and mitochondria promotes release of stored Ca^{2+} and pro-apoptotic proteins (cytochrome c, SMAC/DIABLO, AIF, etc.) into the cytosol [71]. In general, severe oxidative stress causes necrosis, whereas moderate stress can elicit apoptosis that predominate in the ischemic core and penumbra, respectively. The simultaneous degeneration of neurons, glial cells, and capillaries, and development of vasogenic and intracellular edema in the infarction core were observed at 4 h after PTS in the rat cerebral cortex at the histological and ultrastructural levels [40, 47].

Photothrombotic infarct was suggested to be the result of occlusive vascular thrombosis due to platelet aggregation and platelet-endothelium interaction [22, 34, 35]. Emboli may be carried distally from the site of photoinjury and cause multiple cerebral infarction [35]. However, the primary mechanisms of PTS, the links between ROS generation and platelet aggregation are not well understood. The role of platelet aggregation in PTS is debated. On one hand, platelet aggregation and platelet-containing thrombi were observed in many cases of cerebral photothrombosis [34, 35, 47]. Different anti-platelet drugs reduced the photothrombotic brain damage. For example, the selective phosphodiesterase 3 inhibitor K-134, which has a strong anti-platelet and anti-thrombotic activity, prevented cerebral infarction associated with platelet hyperaggregability under PTS-MCAO [72]. On the other hand, some authors showed that platelet aggregation and clot formation, although occur at PTS, may be not critical for damage of the nervous tissue. The application of some anti-platelet agents and anticoagulants did not reduce significantly the infarct volume and cell damage after PTS. Besides, the size and extent of photothrombotic brain damage did not change in mice with the deficiency of platelets and coagulation factors [73, 74]. Therefore, the mechanism of PTS-induced tissue damage can differ from that in human stroke, where platelet aggregation and blood clotting factors are the major pathogenic factors.

Both cytotoxic and vasogenic edema are significant components of photothrombotic brain injury [40, 45–47]. In human stroke, however, tissue infarct is mainly associated with cytotoxic edema, whereas vasogenic edema develops several hours later [20, 45]. Brain edema contributes to reduction of the infarct volume [45]. In PTS, both edema types were observed at as early as 1–4 h after light exposure [40, 46, 47]; however, their mechanisms may be different. The cytotoxic edema is apparently the result of acute oxygen and energy deprivation, deterioration of active ion pumping, impairment of ionic homeostasis, loss of cellular osmoregulation, swelling of intracellular organelles, and massive vacuolization of the

cytoplasm. The increased Na^+ influx induces osmotic movement of water into neurons and glial cells through aquaporins that leads to organelle and cell swelling and brain edema [61]. In PTS, massive vascular leakage inside the infarct core occurred within the first hour after light exposure. This flow was reduced at 4 h, but a substantial leakage was still maintained in the penumbra at 24 h after PTS [75]. Rapid water influx is followed by necrotic cell lysis, especially in the ischemic core [20, 76]. Thus, both occlusive thrombi and vascular leakage are the pathogenic factors in photothrombotic stroke. The development of focal cerebral ischemia in rats was shown to be associated with the activity of Na^+/H^+ exchanger; its inhibition reduced the infarct volume [77].

The vasogenic edema is associated with PTS-induced BBB breakdown [45–47]. These processes occur shortly, at 1–4 h after photothrombotic lesion [34, 46, 47, 78]. As a consequence of BBB disruption, some PS molecules can penetrate glia and neurons and contribute to direct photodynamic injury of these cells [79]. Acute vasogenic edema is associated with release of proteolytic enzymes from necrotic cells, which degrade the extracellular matrix and cellular membranes [47]. Caveolin-1 is a key modulator of vascular permeability. It played a critical role in the regulation of blood-brain barrier permeability after focal ischemic injury [80]. The comparative study of PTS-induced changes in the O_2^- level, oxidative DNA damage, BBB integrity and infarct volume in the wild-type mice and transgenic mice, which over-express Cu/Zn superoxide dismutase, showed that PTS-induced BBB disruption is mediated by O_2^-. The cytosolic Cu/Zn superoxide dismutase protected brain from BBB disruption and infarction after PTS [81].

PTS-Induced Penumbra

The ischemic penumbra is not initially inured. It is considered as a potentially salvageable tissue. The main interest in the ischemic stroke research is the mechanisms that control penumbra formation, and search of neuroprotective agents capable to inhibit this process and to save neuronal cells in this peri-infarct zone.

How to visualize the ischemic penumbra? Traditional hematoxylin/eosin straining shows the basic morphological alterations in cells surrounding the necrotic core with an optical spatial resolution of 1–2 μm. It has been used in many past studies. Electron microscopy shows fine ultrastructural changes in the cellular components with much better spatial resolution—about 2–5 nm [40]. The immunohistochemical methods visualize the distribution of various proteins in the cerebral tissue. Some of them, such as c-fos and HSP-90 served as penumbra markers [48]. Another potential penumbra marker is astrocytes-specific glial fibrillary acidic protein (GFAP) that indicates gliosis and formation of glial scar [82]. However, these methods require fixed tissue samples and cannot be applied to humans and living animals.

Magnetic resonance imaging is the gold standard in noninvasive studies of global alterations in the brain structure of experimental animals or humans in a clinic. Defining the ischemic penumbra allows selection of patients suitable for recanalization therapy in clinic [48]. MRI variants such as perfusion-weighted imaging (PWI), diffusion-weighted imaging (DWI), and T2-weighted imaging (T2WI) were used to determine the infarct volume and to visualize the ischemic penumbra after PTS [45–48, 82]. DWI showed that the lesion core was surrounded by the periphery with distinct apparent diffusion coefficient (ADC) values at 4 h after PTS. These changes were similar to those observed after MCAO in animals and human stroke [47]. The mismatch between the PWI pattern and the ADC map defined the penumbra in mice at different time intervals from 1 to 24 h after MCAO-PTS [48]. However, the spatial resolution of MRI (about 100 μm) is not sufficient for detailed analysis of the tissue lesion.

A novel multi-modal approach to imaging of molecular and elemental alterations in ischemic stroke has been recently developed. In this approach, the traditional methods such as histology, immunohistochemistry, and MRI were complemented with a number of spectroscopic imaging techniques including Fourier transform infrared imaging (global FTIR imaging and single-beam wide-field SR-FTIR imaging with the spatial resolution of 20 and 2–5 μm, respectively), Raman spectroscopic imaging (resolution 0.5 μm), and Coherent anti-Stokes Raman spectroscopy (CARS). These techniques provide the information on the distribution of lipid acyl groups, lipid esters, total protein and aggregated protein content in cells and tissue. X-ray fluorescence imaging (XFI) shows the distribution of various metals (K, Ca, Fe, and Cu–Zn) in the tissue. Using this platform, the authors characterized the peri-infarct zone (i.e., ischemic penumbra) at 24 h after BR-PTS in the mouse brain cortex. They suggested that the photothrombotic ischemic model may be highly valuable to study the biochemical mechanisms of edema following ischemic insult and to test the efficacy of novel treatments aimed at minimizing edema [82].

Another approach to multi-modal characterization of the PTS results in the mouse or rat brain included the combination of the histological hematoxylin/eosin staining; delineation of infarct area by triphenyl tetrazolium chloride (TTC) staining; immunohistochemical staining for anti-alpha smooth muscle actin, GFAP, CD68, and NeuN; regional cerebral vasculature examination by LSCI; assessment of blood-brain barrier disruption using Evans blue; T2WI, DWI, and PWI magnetic resonance imaging; and evaluation of cerebral glucose metabolism by micro-positron emission tomography/computer tomography imaging (MicroPET/CT). Using this complex approach, tissue infarct, brain edema and BBB disruption were observed in the infarction core in the first day after PTS.

Neovascularization started at day 3, whereas astroglial and inflammation response involving macrophages and microglia – at day 7. The gradual increase in the number of inflammatory cells and astrocytes, neovascularization, recoverable improvement of BBB permeability, CBF, and glucose metabolism were demonstrated in the peri-infarct region rather than in the infarct core [45].

A major criticism of the PTS model is little or no salvageable penumbra due to intense development of necrosis in the infarction core. This reduces the translational efficacy of this stroke model for search of neuroprotective agents capable to save the penumbra cells.

In order to study neurodegeneration and neuroprotection in the ischemic penumbra, some modifications of the photothrombotic model have been developed. Less intense but prolonged photodynamic action (Rose Bengal; 532 nm laser irradiation, 60 mW/cm^2, 30 min) induced the 1.5–2 mm width penumbra around the 3-mm infarction core in the rat cerebral cortex. This was confirmed by histological and electron-microscopic studies. The ultrastructural alterations in the peri-infarct area adjacent to the PTS core in the rat cerebral cortex were similar but slightly weaker than in the infarct core. They included significant cytotoxic and vasogenic edema, pyknosis and karyopyknosis, destruction of intracellular organelles, and other hallmarks of degeneration of neurons, glial cells, and capillaries. These morphological changes decreased gradually across the penumbra. The ischemic penumbra has not a distinct boundary. At a distance of about 1.5 mm from the infarction core, the cortical morphology looked almost normal, except the vasogenic edema around some vessels and neurons [40].

Other authors also observed the mild diffuse peri-infarct injury in the rat cerebral cortex around the ischemic infarct core that was induced by PTS with the reduced RB dose (10 mg/kg) and low white light intensity (40 mW/cm^2, 555 nm, 5 min) [83]. Nahirney et al. (2016) reported that the PTS-induced break of BBB occurred not only in the infarct core, but also in the peri-infarct zone. End feet of astrocytes and their mitochondria were severely swollen at 3 h after PTS. These changes were partially recovered by 72 h. BBB permeability was associated with an occurrence of endothelial caveolae and vacuoles, rather than with loss of tight junctions [84]. BBB opening and extravasation of albumin was suggested to facilitate K^+-mediated spreading depolarization associated with epileptiform discharges in the penumbra [85].

In the "ring" PTS model, the argon laser beam (514.5 nm, 0.9 W/cm^2, 2 min; photosensitizer erythrosine B) was configured as the narrow ring with 5-mm diameter and 0.35-mm width. The advantage of this model is the anatomically predefined region at-risk (ischemic penumbra) inside the circle surrounded by the ring of necrotic tissue. The local cerebral blood flow inside the photothrombotic ring declined promptly after irradiation. This mimicked the ischemic penumbra. In the central region, some neurons swelled at 4 h after ring-PTS. Neuronal necrosis, neuropil damage, and progressive formation of cystic cavities were observed at 24 h. At 48 h, the majority of neurons were severely swollen, eosinophilic, and pyknotic. However, at 7 days after PTS, the tissue morphology partly normalized [86–88].

Extracellular acidosis is an important consequence of ischemic stroke. It activates Na^+/H^+ exchanger isoform 1 (NHE1) in the central nervous system pericytes. NHE1 affects the endoplasmic reticulum and thereby causes Ca^{2+} oscillations. The repetitive increase in cytosolic Ca^{2+} mediates phosphorylation of CaMKII that translocates into the nucleus and phosphorylates CREB, which further initiates transcription of genes that encode a variety of proteins [89].

Necrotic cell death dominates in the PTS core, whereas in the penumbra apoptosis prevails [90, 91]. The ratio of apoptotic and necrotic cells in the penumbra (~ 1:2) was maintained up to 72 h after PTS. In penumbra regions adjacent to the infarct core, the highest level of apoptotic cells was observed at 24 h after PTS, whereas the peak amount of necrotic cells was observed later at 48 h [92]. Repair of the damaged brain tissue and filling this area with neurons and glial cells occurred from 3 to 28 days [93]. Elevated level of apoptosis in the penumbra after PTS was characterized with overexpression of p53, de-novo protein synthesis and endonuclease-mediated DNA injury [94]. The over-expression of anti-apoptotic proteins Bcl-w and Bcl-2 and relatively unchanged levels of pro-apoptotic proteins Bax and SMAC/DIABLO were observed at 4–72 h after low-intensity ring PTS. At 1–24 h after highly intense irradiation, Bcl-w level decreased and Bcl-2 level increased. SMAC/DIABLO released from mitochondria to the cytosol and induced massive apoptosis. Therefore, the intensity of PTS-induced focal ischemia determines the balance between anti- and pro-apoptotic proteins and, correspondingly, cell survival or death [92].

The proteomic study using antibody microarrays showed the complex regulation of pro- and anti-apoptotic processes in the penumbra that surrounds the PTS-induced ischemic core in the rat cerebral cortex. The changes in protein expression were greatest at 4 h after PTS comparing with 1 or 24 h. At this time, over-expression of proteins that initiate and regulate diverse proapoptotic pathways (Par4, E2F1, p75, p38, JNK, c-myc, p53, GADD153, GAD65/67, and NMDAR2a) and execute the apoptosis program (AIF, SMAC/DIABLO, Bcl-10, PSR, caspases 3, 6, and 7) was observed. Simultaneously, different antiapoptotic proteins (Bcl-x, p63, p21WAF-1, MDM2, ERK5, MKP-1, NEDD8, and estrogen receptor) were up-regulated. Over-expression of Ca^{2+}-dependent (calmodulin, CaMKIIα, and CaMKIV) and other signaling proteins (ERK1/2, MAKAPK2, PKBα, RAF1, protein phosphatase 1α, ATF2, DYRK1A, and EGF receptor) in the penumbra versus the contralateral cortex of the same animals might participate in the anti-apoptotic processes. At the same time, other

signaling proteins such as Notch/NUMB, TDP43, or components of the Wnt/β-catenin pathway (axin1, GSK-3, and FRAT1) were down-regulated. Down-regulation of Cdk6, Cdc7 kinase, Trf1, and topoisomerase-1 could be related to the suppression of proliferation [40, 41].

Overexpression of proteins that regulate axon outgrowth and guidance (NAV-3, CRMP2, and PKCβ2), intercellular interactions (N-cadherin, PMP22), mitochondria quality control (Pink1, parkin), ubiquitin-mediated proteolysis (ubiquilin-1, UCHL1) and metabolism (LRP1, monoamine oxidase B) was possibly associated with attempts to maintain the integrity of the penumbra tissue. Bidirectional changes in the levels of adhesion and cytoskeleton proteins might be associated with destruction and remodeling of the penumbra tissue. These included up-regulation of different actin-associated proteins (cofilin, actopaxin, p120CTN, α-catenin, p35, and myosin Va and pFAK), whereas other actin-associated proteins (ezrin, spectrin (α+β), tropomyosin, neurofilament 68, and neurofilament-M) as well as components of microtubules and intermediate filaments (β_{IV}-tubulin, polyglutamated β-tubulin, doublecortin, and cytokeratins 7 and 19) were down-regulated. Reduced expression of adaptin β1/2, synip, ALS2, VILIP1, syntaxin, synaptophysin, and synaptotagmin indicated the impairment of vesicular transport and synaptic processes. Simultaneously, proteins involved in dopamine metabolism (tyrosine hydroxylase, DOPA decarboxylase, and dopamine transporter) were down-regulated. On the other hand, some synaptic and vesicular transport proteins (syntaxin-8, TMP21, Munc-18-3, tryptophan hydroxylase, and glutamate decarboxylase) were upregulated [40].

Such concerted expression in the penumbra of various pro- and antiapoptotic proteins, which control very different aspects of the complex tissue reaction, remains to be understood. The signaling pathways leading from the primary pathogenic agents, which propagate the ischemic lesion to surrounding tissue (glutamate, Ca^{2+}, spreading depolarization, ROS, acidosis, edema, etc.) to transcription factors that regulate expression of these proteins are still unknown. One can suggest the pivotal role of some signaling proteins (such as p38 and p53) and transcription factors (such as E2F1, HIF-1α, and p53) in regulation of apoptosis in the penumbra [41, 92, 95]. The causative relationships between expression of transcription factor HIF-1α and induction of caspase 3 in the penumbra was observed in the rat brain at 12 and 24 h after PTS [96].

Taken together, these data provide the integral view on the molecular basis of neurodegeneration, neuroprotection, and tissue remodeling in the penumbra after photothrombotic infarct. Some of these changes are associated with cell injury and death, whereas others are involved in cell survival and protection. The balance between injurious and recovery processes in this area determines the cell fate [40, 41]. Nevertheless, it should be taken into account that these data were averaged over the whole penumbra sample (2-mm ring around 3-mm infarct core) because the proteomic study requires 100–200 mg tissue samples. However, the penumbra is very spatially inhomogeneous with significant injury gradient from the infarct core to periphery. Moreover, it consists of different cell types (neurons, glial cells, vessels, blood cells, etc.), which interact with each other and differently react to injury. So, more detailed study of the potential roles of various proteins in the response of different penumbra elements to PTS is needed.

Nevertheless, some of these proteins may be novel potential targets for the anti-stroke therapy, and some of their inhibitors may be potential anti-stroke neuroprotectors. The PTS model is currently used by different research groups for testing of various anti-stroke medications.

Use of PTS Model in Testing of Potential Neuroprotective Agents

Different anti-stroke strategies and neuroprotective agents that can potentially prevent damage propagation and improve survival of neuronal cells have been tested using the photothrombotic stroke model. In these studies, not only traditional cortical PTS, but other PTS variants such as MCAO-PTS [97, 98] or photothrombotic spinal cord injury [99] were explored. We overview here the data on neuroprotective effects of some drugs that can reduce the acute photothrombotic brain damage within the first 24 h after PTS when neuroprotection is still possible (Table 1). The pharmacological correction of recovery, regeneration, and rehabilitation processes that occur after the first 24 h remains beyond this review.

The first generation of neuroprotective agents was directed to inhibition of calcium channels, glutamate excitotoxicity and oxidative stress. Some of them showed positive effects in the experiments on rats and mice. For example, the application of Ca^{2+} channel blocker diazepam at 1 and 4 h after PTS reduced the infarct volume and protected neuronal cells [100]. Modulation of different potassium channels has attracted attention as a novel strategy to reduce stroke-induced brain injury. The newly discovered potassium channel TREK-1, that is found recently in cerebral neurons, glia, and vascular elements, contributes to the background leak K^+ current. TREK-1 regulates neuronal excitability. It is responsive to various physiological and pathological stimuli such as membrane stretch, intracellular acidification, temperature, and polyunsaturated fatty acids, and plays a key role in neuroprotection after cerebral ischemia. Activation of TREK-1 by α-linolenic acid in a rat brain after PTS exerted the multi-cellular protective effects; it restored the astrocytic glutamate transporter GLT-1, down-regulated aquaporin AQP4, reduced edema and apoptosis and improved behavioral function recovery [101]. Retigabine, an opener of M-type K^+ channel (KCNQ), decreased infarct size, reduced inflammation, and prevented neurological dysfunctions after PTS [98].

Table 1 Some anti-stroke compounds tested using photothrombotic stroke model that showed neuroprotective effects after application within first 24 h after ischemic injury. IS – infarct size

Modality	Substance	Effect	References
Ca^{2+} channel blocker	Diazepam	IS decrease	[100]
Activator of K^+channels TREK-1	α-linolenic acid	Activates potassium channels TREK-1. Hyperpolarizes cells. Reduces expression of aquaporin-4, edema, apoptosis, and activation of microglia; improves functional recovery.	[101]
Opener of M-type K^+ channel (KCNQ)	Retigabine	Decreases IS, inflammation, prevents neurological dysfunctions	[98]
Fe^{2+} chelator, antioxidant	2,2′-dipyridyl	Reduces level of toxic free Fe^{2+}, production of ROS, expression of HO-1and HIF-1α, apoptosis, and IS.	[102–104]
NMDAR antagonists	Memantine	Improves stroke outcome, decreases astrogliosis, increases levels of BDNF at oral administration	[105]
	1-metho-xyoctadecan-1-ol	Reduces IS, edema, improves functional outcome	[106]
Antioxidant, mitochondria protection	ITH33/IQM9.21	Multi-target effects: antioxidant, protects mitochondria, reduces Ca^{2+} level, protects neurons in penumbra, decreases IS	[107]
Antioxidant	Melatonin	Inhibits MMP-9 and attenuates BBB disruption, reduces risk of t-PA-mediated hemorrhage. Reduces IS and functional deficit, improves motor skills. Effects are mediated by HO-1 and nicotinic nAcChR	[98, 99, 108–110]
Downregulates MMP-9	Rutin	Attenuates PTS-induced MMP-9 activation and disruption of BBB; improves functional outcome	[111]
MMP inhibitors	Minocycline Doxycycline Batimastat	Reduce IS; decrease expression of MCP-1, TNF-α, and IDO	[112]
α7 nAChR agonist	PNU282987	Affects Nrf2/HO-1 pathway; reduces ROS production, TNF release and cell death, induces HO-1 expression. Decreases IS, improves motor skills.	[113]
Activation of Nrf2	Sulforaphane	Increases transcription of Nrf2, Hmox1, GCLC and GSTA4 mRNA	[114]
Neurotrophic factor	BDNF	Induces neuronal remodeling; reduces pathological astrogliosis, improves functional motor recovery	[115, 116]
Inhibitor of transglutaminases	Cystamine	Increases level of BDNF, neuronal survival and plasticity, induces functional recovery, regulates axon remodeling, and enhances neuronal progenitor cell proliferation	[117]
Soluble Nogo66 receptor	sNgR-FC	Prevents PTS-induced up-regulation of RhoA, p-JNK, p-c-JUN and p-ATF-2 in ipsilateral hemisphere via inhibition of RhoA/JNK pathway	[118]
Serotonin reuptake inhibitors	Fluoxetine, Sertraline	Reduces IS, normalizes blood pressure, via increased expression of HO-1, HIF-1α in ischemic core	[119]
Erythropoietin	Carbamylated derivatives	Reduce IS, nootropic and neuroprotective effects	[120]
Extra-low frequency electromagnetic field		Neuroprotective effect. Up-regulation of BDNF, TrkB, pAkt, Bcl-xL, and pBad after PTS; down-regulation of Bad, Bax and caspase 3, IL1β and MMP9	[121]

The level of cytotoxic Fe^{2+} in the infarct core and penumbra increased after the PTS. Iron chelator ferritin was also up-regulated in these regions. Application of Fe^{2+} chelator and antioxidant 2,2′-dipyridyl reduced the level of toxic-free Fe^{2+},

decreased production of ROS, and expression of HO-1 and HIF-1α. As a result, PTS-induced apoptosis was inhibited, brain lesion and ischemic volume decreased. These data showed the importance of the iron chelation therapy very soon after ischemic stroke [102–104].

Different inhibitors of glutamate NMDA receptors such as MK-801 also reduced photothrombotic brain damage in animals, but could not be used for human treatment because of strong adverse effects. The safer next generation anti-excitotoxic agents such as memantine [105] or 1-methoxyoctadecan-1-ol [106] reduced the infarct volume and functional deficit without such negative effects. After oral administration, memantine increased the expression of BDNF, reduced reactive astrogliosis, and stimulated vascularization in the penumbra. It improved recovery of sensory and motor cortical functions. The clinical availability and tolerability of memantine make it to be a potential candidate for clinical translation [105].

Multi-target ligands may be more efficient than a single-targeted compound. Lorrio et al. (2013) used the glutamic acid derivative ITH33/IQM9.21, which blocks voltage-dependent Ca^{2+} current and reduces the transient elevation of $[Ca^{2+}]_c$ that is elicited by depolarizing stimuli. Its i.p. injection before and during 2 days after PTS caused twofold decrease in the infarct volume in the mouse brain. The neuroprotective effect of ITH33/IQM9.21 on vulnerable neurons in the ischemic penumbra could be associated with reduction of Ca^{2+} overload, mitochondrial protection and antioxidant action [107].

Melatonin, a pineal secretory hormone, is a potent antioxidant and radical scavenger. Its application induced multiple beneficial effects in the PTS-treated animals. It maintained the penumbral blood flow, reduced the PTS-induced infarction zone, improved functional outcome and motor skills [99, 108, 109]. These effects were possibly mediated by cyclooxygenase 1 [108], heme oxygenase-1, and α7 nicotinic acetylcholine receptors (α7 nAChR) [109]. Melatonin attenuated photothrombotic disruption of BBB via inhibition of matrix metalloproteinase-9 (MMP-9), which disrupts BBB [97, 99, 110], and reduced risk of t-PA-mediated hemorrhage [97]. Similarly, rutin down-regulated MMP-9, suppressed PTS-induced disruption of BBB; and improved functional outcome after PTS [111]. Other inhibitors of matrix metalloproteinases minocycline, doxycycline, and batimastat also reduced the cerebral infarct volume that could be associated with down-regulation of a number of signaling molecules such as monocyte chemotactic protein-1 (MCP-1), tumor necrosis factor-α (TNF-α), and indoleamine 2,3-dioxygenase (IDO) [112].

Using PNU282987, an agonist of α7 nAChR, which affects Nrf2/HO-1 pathway and induces HO-1 expression, decreased ischemic volume, improved motor skills, reduced ROS production, TNF release and cell death [113]. The transcription factor Nrf2 controls expression of various proteins involved in the antioxidant cell protection. Its activation by sulforaphane increased transcription of Nrf2, Hmox1, GCLC, and GSTA4 in the mouse brain and exerted neuroprotective action in the photothrombotic cerebral ischemia, but did not influence the infarct volume, the number of activated glial cells, and improvement of animal motor function [114].

PTS was shown to induce an early and transient over-expression of brain-derived neurotrophic factor (BDNF) not only in the injured cortical region but generally in both hemispheres at 4 h after the impact, and later, from 8 to 30 days, in hippocampus. This suggests the involvement of BDNF in post-stroke plasticity [115]. Post-PTS administration of BDNF did not reduce; however, the infarct volume, but improved functional motor recovery, reduced pathological astrogliosis, and induced widespread neuronal remodeling [116]. Cystamine, an inhibitor of transglutaminases, has been demonstrated to exert the neuroprotection effect in neurodegenerative diseases. Its application at 24 h after PTS resulted in improvement of impaired functional activity, axon remodeling, enhanced neuronal survival and plasticity, and proliferation of neuronal progenitor cells in mice. These effects might be associated with up-regulation of BDNF and phosphorylation of its receptor TrkB [117].

Other signaling pathways also regulate the brain responses to PTS. For example, soluble Nogo66 receptor sNgR-FC prevented PTS-induced increase in the levels of RhoA, p-JNK, p-c-JUN and p-ATF-2 in ipsilateral hemisphere via inhibition of RhoA/JNK pathway. This suggests that sNgR-Fc can mitigate axonal injury after photothrombotic cortical infarction through suppression of RhoA/JNK signaling pathways [118]. Inhibitors of serotonin reuptake fluoxetine or sertraline reduced the PTS-induced infarct volume and normalized blood pressure through over-expression of HO-1, HIF-1α in the ischemic core [119]. Intraperitoneal injection of erythropoietin or its carbamylated derivatives (EPO-Fc and EPO-TR fusion proteins) at 1 h after bilateral PTS reduced infarction size and exerted nootropic and neuroprotective effects [120].

The most of these drugs have been also tested on other stroke models and after showing promising results are under clinical trials [8, 9, 122].

Not only pharmacological but also physical factors can exert a neuroprotective effect on the animal brain after PTS. For example, extra-low frequency pulsed electromagnetic field (60 Hz; 10 mT) activated the prosurvival BDNF/TrkB/Akt signaling pathway in the mouse brain during the recovery period after PTS. The authors observed up-regulation of BDNF, TrkB, pAkt, Bcl-xL, and pBad at 3 and 14 days after PTS, whereas the levels of proapoptotic proteins Bad, Bax and caspase 3, proinflammatory mediator IL1β, and matrix metalloprotease MMP9 decreased. Such non-chemical methods of modulating neurological and psychological functions are of growing interest because they are non-invasive, inexpensive, and safe [121].

Conclusion

Photothrombotic stroke is the unique model of occlusion of small cerebral vessels. In comparison with other stroke models, its advantages include well-defined location of an ischemic lesion that is determined by the aiming of the laser beam at the predetermined brain region, the degree of ischemic lesion is determined by light intensity and duration, the lesion is well reproducible due to the stereotaxic accuracy of irradiation and continuous monitoring of light intensity, and low invasiveness and minimal surgical intervention. PTS does not require craniotomy and mechanical manipulations with blood vessel such as ligation or filament insertion, which carry the risk of local brain trauma; low animal mortality (< 10%); prolonged sensorimotor impairment that provides long-term study of stroke consequences and behavior impairment and recovery; and independence on genetic variations of blood pressure and vascular architecture. However, disadvantages of this stroke model include some differences from the ischemic stroke pathology in humans such as strong edema and very narrow penumbra. Nevertheless these drawbacks can be reduced in some PTS variations. PTS is currently used for examination of the neuroprotective effects of different potential neuroprotectors. Thus, PTS is the useful and promising experimental model for study of cellular and molecular stroke mechanisms underlying neurodegeneration, neuroprotection, neuroregeneration, and brain plasticity and for search of potential agents capable to treat the stroke consequences.

Funding The work was supported by the Russian Scientific Foundation (# 14-15-00068) and the Ministry of Education and Science of Russian Federation (#6.4951.2017/6.7).

Compliance with Ethical Standards

Conflict of Interest The author declares that there is no conflict of interests.

Ethical Approval This article does not contain any studies with human participants or animals performed by the author.

References

1. Holloway PM, Gavins FN. Modeling ischemic stroke in vitro: status quo and future perspectives. Stroke. 2016;47(2):561–9. https://doi.org/10.1161/STROKEAHA.115.011932.
2. Auriel E, Bornstein NM. Neuroprotection in acute ischemic stroke-current status. J Cell Mol Med. 2010;14(9):2200–2. https://doi.org/10.1111/j.1582-4934.2010.01135.x.
3. Iadecola C, Anrather J. Stroke research at a crossroad: asking the brain for directions. Nat Neurosci. 2011;14(11):1363–8. https://doi.org/10.1038/nn.2953.
4. O'Collins VE, Macleod MR, Donnan GA, Horky LL, van der Worp BH, Howells DW. 1,026 experimental treatments in acute stroke. Ann Neurol. 2006;59(3):467–77. https://doi.org/10.1002/ana.20741.
5. Ginsberg MD. Neuroprotection for ischemic stroke: past, present and future. Neuropharmacology. 2008;55(3):363–89. https://doi.org/10.1016/j.neuropharm.2007.12.007.
6. Jain KK. The handbook of neuroprotection. New York: Springer Science + Business Media; 2011. https://doi.org/10.1007/978-1-61779-049-2.
7. Muresanu DF, Buzoianu A, Florian SI, von Wild T. Towards a roadmap in brain protection and recovery. J Cell Mol Med. 2012;16(12):2861–71. https://doi.org/10.1111/j.1582-4934.2012.01605.x.
8. Min J, Farooq MU, Gorelick PB. Neuroprotective agents in ischemic stroke: past failures and future opportunities. Clin Invest. 2013;3(12):1167–77. https://doi.org/10.4155/cli.13.91.
9. Majid A. Neuroprotection in stroke: past, present, and future. ISRN Neurol. 2014;2014:515716. https://doi.org/10.1155/2014/515716.
10. Karsy M, Brock A, Guan J, Taussky P, Kalani MY, Park MS. Neuroprotective strategies and the underlying molecular basis of cerebrovascular stroke. Neurosurg Focus. 2017;42(4):E3. https://doi.org/10.3171/2017.1.FOCUS16522.
11. Rajah GB, Ding Y. Experimental neuroprotection in ischemic stroke: a concise review. Neurosurg Focus. 2017;42(4):E2. https://doi.org/10.3171/2017.1.FOCUS16497.
12. Mehta SL, Manhas N, Raghubir R. Molecular targets in cerebral ischemia for developing novel therapeutics. Brain Res Rev. 2007;54(1):34–66. https://doi.org/10.1016/j.brainresrev.2006.11.003.
13. Puyal J, Ginet V, Clarke PG. Multiple interacting cell death mechanisms in the mediation of excitotoxicity and ischemic brain damage: a challenge for neuroprotection. Prog Neurobiol. 2013;105:24–48. https://doi.org/10.1016/j.pneurobio.2013.03.002.
14. Krafft PR, Bailey EL, Lekic T, Rolland WB, Altay O, Tang J, et al. Etiology of stroke and choice of models. Int J Stroke. 2012;7(5):398–406. https://doi.org/10.1111/j.1747-4949.2012.00838.x.
15. Sommer CJ. Ischemic stroke: experimental models and reality. Acta Neuropathol. 2017;133(2):245–61. https://doi.org/10.1007/s00401-017-1667-0.
16. Mergenthaler P, Meisel A. Do stroke models model stroke? Dis Model Mech. 2012;5(6):718–25. https://doi.org/10.1242/dmm.010033.
17. Bacigaluppi M, Comi G, Hermann DM. Animal models of ischemic stroke. Part two: modeling cerebral ischemia. Open Neurol J. 2010;4(2):34–8. https://doi.org/10.2174/1874205X01004020034.
18. Woodruff TM, Thundyil J, Tang SC, Sobey CG, Taylor SM, Arumugam TV. Pathophysiology, treatment, and animal and cellular models of human ischemic stroke. Mol Neurodegener. 2011;6(1):11. https://doi.org/10.1186/1750-1326-6-11.
19. Fluri F, Schuhmann MK, Kleinschnitz C. Animal models of ischemic stroke and their application in clinical research. Drug Des Devel Ther. 2015;9:3445–54. https://doi.org/10.2147/DDDT.S56071.
20. Carmichael ST. Rodent models of focal stroke: size, mechanism, and purpose. Neuro Rx. 2005;2(3):396–409. https://doi.org/10.1602/neurorx.2.3.396.
21. Toyota S, Graf R, Valentino M, Yoshimine T, Heiss WD. Malignant infarction in cats after prolonged middle cerebral artery occlusion: glutamate elevation related to decrease of cerebral perfusion pressure. Stroke. 2002;33(5):1383–91. https://doi.org/10.1161/01.STR.0000015557.18508.DD.
22. Watson BD, Dietrich WD, Busto R, Wachtel MS, Ginsberg MD. Induction of reproducible brain infarction by photochemically initiated thrombosis. Ann Neurol. 1985;17(5):497–504. https://doi.org/10.1002/ana.410170513.

23. Uzdensky AB. Cellular and molecular mechanisms of photodynamic therapy. Sankt-Petersburg: Nauka; 2010. (in Russian)
24. Yoo JO, Ha KS. New insights into the mechanisms for photodynamic therapy-induced cancer cell death. Int Rev Cell Mol Biol. 2012;295:139–74. https://doi.org/10.1016/B978-0-12-394306-4.00010-1.
25. Kessel D. Apoptosis and associated phenomena as determinants of the efficacy of photodynamic therapy. Photochem Photobiol Sci. 2015;14(8):1397–402. https://doi.org/10.1039/c4pp00413b.
26. Benov L. Photodynamic therapy: current status and future directions. Med Princ Pract. 2015;24(Suppl 1):14–28. https://doi.org/10.1159/000362416.
27. Allison RR, Moghissi K. Oncologic photodynamic therapy: clinical strategies that modulate mechanisms of action. Photodiagn Photodyn Ther. 2013;10(4):331–41. https://doi.org/10.1016/j.pdpdt.2013.03.011.
28. Bechet D, Mordon SR, Guillemin F, Barberi-Heyob MA. Photodynamic therapy of malignant brain tumours: a complementary approach to conventional therapies. Cancer Treat Rev. 2014;40(2):229–41. https://doi.org/10.1016/j.ctrv.2012.07.004.
29. Quirk BJ, Brandal G, Donlon S, Vera JC, Mang TS, Foy AB, et al. Photodynamic therapy (PDT) for malignant brain tumors—where do we stand? Photodiagn Photodyn Ther. 2015;12(3):530–44. https://doi.org/10.1016/j.pdpdt.2015.04.009.
30. Garland MJ, Cassidy CM, Woolfson D, Donnelly RF. Designing photosensitizers for photodynamic therapy: strategies, challenges and promising developments. Future Med Chem. 2009;1(4):667–91. https://doi.org/10.4155/fmc.09.55.
31. Uzdensky AB, Ma LW, Iani V, Hjortland GO, Steen HB, Moan J. Intracellular localisation of hypericin in human glioblastoma and carcinoma cell lines. Lasers Med Sci. 2001;16(4):276–83. https://doi.org/10.1007/PL00011364.
32. Chen B, Pogue BW, Hoopes PJ, Hasan T. Vascular and cellular targeting for photodynamic therapy. Crit Rev Eukaryot Gene Expr. 2006;16(4):279–305. https://doi.org/10.1615/CritRevEukarGeneExpr.v16.i4.10.
33. Schmitt F, Juillerat-Jeanneret L. Drug targeting strategies for photodynamic therapy. Anti Cancer Agents Med Chem. 2012;12(5):500–25. https://doi.org/10.2174/187152012800617830.
34. Dietrich WD, Busto R, Watson BD, Scheinberg P, Ginsberg MD. Photochemically induced cerebral infarction. II. Edema and blood–brain barrier disruption. Acta Neuropathol (Berl). 1987;72(4):326–34. https://doi.org/10.1007/BF00687263.
35. Ishikawa M, Sekizuka E, Oshio C, Sato S, Yamaguchi N, Terao S, et al. Platelet adhesion and arteriolar dilation in the photothrombosis: observation with the rat closed cranial and spinal windows. J Neurol Sci. 2002;194(1):59–69. https://doi.org/10.1016/S0022-510X(01)00673-6.
36. Seery VL, Morgan WT, Muller-Eberhard U. Interaction of rabbit hemopexin with rose bengal and photooxidation of the rose bengal-hemopexin complex. J Biol Chem. 1975;250(16):6439–44.
37. Markgraf CG, Kraydieh S, Prado R, Watson BD, Dietrich WD, Ginsberg MD. Comparative histopathologic consequences of photothrombotic occlusion of the distal middle cerebral artery in Sprague-Dawley and Wistar rats. Stroke. 1993;24(2):286–92. https://doi.org/10.1161/01.STR.24.2.286.
38. Alaverdashvili M, Paterson PG, Bradley MP. Laser system refinements to reduce variability in infarct size in the rat photothrombotic stroke model. J Neurosci Methods. 2015;247:58–66. https://doi.org/10.1016/j.jneumeth.2015.03.029.
39. Demyanenko SV, Panchenko SN, Uzdensky AB. Expression of neuronal and signaling proteins in penumbra around a photothrombotic infarction core in rat cerebral cortex. Biochem Mosc. 2015;80(6):790–9. https://doi.org/10.1134/S0006297915060152.
40. Uzdensky A, Demyanenko S, Fedorenko G, Lapteva T, Fedorenko A. Photothrombotic infarct in the rat brain cortex: protein profile and morphological changes in penumbra. Mol Neurobiol. 2017;54(6):4172–88. https://doi.org/10.1007/s12035-016-9964-5.
41. Demyanenko S, Uzdensky A. Profiling of signaling proteins in penumbra after focal photothrombotic infarct in the rat brain cortex. Mol Neurobiol. 2017;54(9):6839–56. https://doi.org/10.1007/s12035-016-0191-x.
42. Song H, Park JY, Kim HS, Lee MC, Kim Y, Kim HI. Circumscribed capsular infarct modeling using a photothrombotic technique. J Vis Exp. 2016;(112) https://doi.org/10.3791/53281.
43. Labat-gest V, Tomasi S. Photothrombotic ischemia: a minimally invasive and reproducible photochemical cortical lesion model for mouse stroke studies. J Vis Exp. 2013;76. doi: https://doi.org/10.3791/50370.
44. Talley Watts L, Zheng W, Garling RJ, Frohlich VC, Lechleiter JD. Rose Bengal photothrombosis by confocal optical imaging in vivo: a model of single vessel stroke. J Vis Exp. 2015;100:e52794. https://doi.org/10.3791/52794.
45. Liu NW, Ke CC, Zhao Y, Chen YA, Chan KC, Tan DT, et al. Evolutional characterization of photochemically induced stroke in rats: a multimodality imaging and molecular biological study. Transl Stroke Res. 2017;8(3):244–56. https://doi.org/10.1007/s12975-016-0512-4.
46. Chen F, Suzuki Y, Nagai N, Jin L, Yu J, Wang H, et al. Rodent stroke induced by photochemical occlusion of proximal middle cerebral artery: evolution monitored with MR imaging and histopathology. Eur J Radiol. 2007;63(1):68–75. https://doi.org/10.1016/j.ejrad.2007.01.005.
47. Lee VM, Burdett NG, Carpenter A, Hall LD, Pambakian PS, Patel S, et al. Evolution of photochemically induced focal cerebral ischemia in the rat magnetic resonance imaging and histology. Stroke. 1996;27(11):2110–9. https://doi.org/10.1161/01.STR.27.11.2110.
48. Qian C, Li PC, Jiao Y, Yao HH, Chen YC, Yang J, et al. Precise characterization of the penumbra revealed by MRI: a modified photothrombotic stroke model study. PLoS One. 2016;11(4):e0153756. https://doi.org/10.1371/journal.pone.0153756.
49. Yao H, Ibayashi S, Sugimori H, Fujii K, Fujishima M. Simplified model of krypton laser-induced thrombotic distal middle cerebral artery occlusion in spontaneously hypertensive rats. Stroke. 1996;27(2):333–6. https://doi.org/10.1161/01.STR.27.2.333.
50. Parthasarathy AB, Kazm SM, Dunn AK. Quantitative imaging of ischemic stroke through thinned skull in mice with Multi Exposure Speckle Imaging. Biomed Opt Express. 2010;1(1):246–59. https://doi.org/10.1364/BOE.1.000246.
51. Liu Q, Li Y, Lu H, Tong S. Real-time high resolution laser speckle imaging of cerebral vascular changes in a rodent photothrombosis model. Biomed Opt Express. 2014;5(5):1483–93. https://doi.org/10.1364/BOE.5.001483.
52. Kuroiwa T, Xi G, Hua Y, Nagaraja TN, Fenstermacher JD, Keep RF. Development of a rat model of photothrombotic ischemia and infarction within the caudoputamen. Stroke. 2009;40(1):248–53. https://doi.org/10.1161/STROKEAHA.108.527853.
53. Kim HS, Kim D, Kim RG, Kim JM, Chung E, Neto PR, et al. A rat model of photothrombotic capsular infarct with a marked motor deficit: a behavioral, histologic, and microPET study. J Cereb Blood Flow Metab. 2014;34(4):683–9. https://doi.org/10.1038/jcbfm.2014.2.
54. Schaechter JD, Kraft E, Hilliard TS, Dijkhuizen RM, Benner T, Finklestein SP, et al. Motor recovery and cortical reorganization after constraint-induced movement therapy in stroke patients: a preliminary study. Neurorehabil Neural Repair. 2002;16(4):326–33. https://doi.org/10.1177/154596830201600403.

55. Moon SK, Alaverdashvili M, Cross AR, Whishaw IQ. Both compensation and recovery of skilled reaching following small photothrombotic stroke to motor cortex in the rat. Exp Neurol. 2009;218(1):145–53. https://doi.org/10.1016/j.expneurol.2009.04.021.
56. Lu H, Li Y, Yuan L, Li H, Lu X, Tong S. Induction and imaging of photothrombotic stroke in conscious and freely moving rats. J Biomed Opt. 2014;19(9):96013. https://doi.org/10.1117/1.JBO.19.9.096013.
57. Yu C-L, Zhou H, Chai A-P, Yang YX, Mao RR, Xu L. Whole-scale neurobehavioral assessments of photothrombotic ischemia in freely moving mice. J Neurosci Methods. 2015;239:100–7. https://doi.org/10.1016/j.jneumeth.2014.10.004.
58. Lapash Daniels CM, Ayers KL, Finley AM, Culver JP, Goldberg MP. Axon sprouting in adult mouse spinal cord after motor cortex stroke. Neurosci Lett. 2009;450(2):191–5. https://doi.org/10.1016/j.neulet.2008.11.017.
59. Harrison TC, Silasi G, Boyd JD, Murphy TH. Displacement of sensory maps and disorganization of motor cortex after targeted stroke in mice. Stroke. 2013;44(8):2300–6. https://doi.org/10.1161/STROKEAHA.113.001272.
60. Hertz L. Bioenergetics of cerebral ischemia: a cellular perspective. Neuropharmacology. 2008;55(3):289–309. https://doi.org/10.1016/j.neuropharm.2008.05.023.
61. Mongin A. Disruption of ionic and cell volume homeostasis in cerebral ischemia: the perfect storm. Pathophysiology. 2007;14(3–4):183–93. https://doi.org/10.1016/j.pathophys.2007.09.009.
62. Leichsenring A, Riedel T, Qin Y, Rubini P, Illes P. Anoxic depolarization of hippocampal astrocytes: possible modulation of P2X7 receptors. Neurochem Int. 2013;62(1):15–22. https://doi.org/10.1016/j.neuint.2012.11.002.
63. Arundine M, Tymianski M. Molecular mechanisms of calcium-dependent neurodegeneration in excitotoxicity. Cell Calcium. 2003;34(4–5):325–37. https://doi.org/10.1016/S0143-4160(03)00141-6.
64. Yamashima T, Oikawa S. The role of lysosomal rupture in neuronal death. Prog Neurobiol. 2009;89(4):343–58. https://doi.org/10.1016/j.pneurobio.2009.09.003.
65. Kirichok Y, Krapivinsky G, Clapham DE. The mitochondrial calcium uni-porter is a highly selective ion channel. Nature. 2004;427(6972):360–4. https://doi.org/10.1038/nature02246.
66. Green DR, Kroemer G. The pathophysiology of mitochondrial cell death. Science. 2004;305(5684):626–9. https://doi.org/10.1126/science.1099320.
67. Nanetti L, Taffi R, Vignini A, Moroni C, Raffaelli F, Bacchetti T, et al. Reactive oxygen species plasmatic levels in ischemic stroke. Mol Cell Biochem. 2007;303(1–2):19–25. https://doi.org/10.1007/s11010-007-9451-4.
68. Abramov AY, Scorziello A, Duchen MR. Three distinct mechanisms generate oxygen free radicals in neurons and contribute to cell death during anoxia and reoxygenation. J Neurosci. 2007;27(5):1129–38. https://doi.org/10.1523/JNEUROSCI.4468-06.2007.
69. Allen CL, Bayraktutan U. Oxidative stress and its role in the pathogenesis of ischemic stroke. Int J Stroke. 2009;4(6):461–70. https://doi.org/10.1111/j.1747-4949.2009.00387.x.
70. Chen H, Yoshioka H, Kim GS, Jung JE, Okami N, Sakata H, et al. Oxidative stress in ischemic brain damage: mechanisms of cell death and potential molecular targets for neuroprotection. Antioxid Redox Signal. 2011;14(8):1505–17. https://doi.org/10.1089/ars.2010.3576.
71. Hayashi T, Saito A, Okuno S, Ferrand-Drake M, Dodd RL, Chan PH. Damage to the endoplasmic reticulum and activation of apoptotic machinery by oxidative stress in ischemic neurons. J Cereb Blood Flow Metab. 2005;25(1):41–53. https://doi.org/10.1038/sj.jcbfm.9600005.
72. Yoshida H, Ashikawa Y, Itoh S, Nakagawa T, Asanuma A, Tanabe S, et al. K-134, a phosphodiesterase 3 inhibitor, prevents brain damage by inhibiting thrombus formation in a rat cerebral infarction model. PLoS One. 2012;7(10):e46432. https://doi.org/10.1371/journal.pone.0046432.
73. Frederix K, Chauhan AK, Kisucka J, Zhao BQ, Hoff EI, Spronk HM, et al. Platelet adhesion receptors do not modulate infarct volume after a photochemically induced stroke in mice. Brain Res. 2007;1185:239–45. https://doi.org/10.1016/j.brainres.2007.07.103.
74. Kleinschnitz C, Braeuninger S, Pham M, Austinat M, Nölte I, Renné T, et al. Blocking of platelets or intrinsic coagulation pathway-driven thrombosis does not prevent cerebral infarctions induced by photothrombosis. Stroke. 2008;39(4):1262–8. https://doi.org/10.1161/STROKEAHA.107.496448.
75. Hoff EI, Egbrink MG, Steinbusch HW, van Oostenbrugge RJ. In vivo visualization of vascular leakage in photochemically induced cortical infarction. J Neurosci Methods. 2005;141(1):135–41. https://doi.org/10.1016/j.jneumeth.2004.06.004.
76. Sattler R, Tymianski M. Molecular mechanisms of calcium-dependent excitotoxicity. J Mol Med. 2000;78(1):3–13. https://doi.org/10.1007/s001090000077.
77. Kitayama J, Kitazono T, Yao H, Ooboshi H, Takaba H, Ago T, et al. Inhibition of Na+/H+ exchanger reduces infarct volume of focal cerebral ischemia in rats. Brain Res. 2001;922(2):223–8. https://doi.org/10.1016/S0006-8993(01)03175-4.
78. Kuroiwa T, Xi G, Hua Y, Nagaraja TN, Fenstermacher JD, Keep RF. Brain edema and blood-brain barrier opening after photothrombotic ischemia in rat. Acta Neurochir Suppl. 2013;118:11–5. https://doi.org/10.1007/978-3-7091-1434-6_2.
79. Gadamski R, Barskow IW, Szumańska G, Wojda R. Blood-brain barrier disturbances and morphological changes in rat brain after photochemically induced focal ischaemia. Folia Neuropathol. 2001;39(3):155–61.
80. Choi KH, Kim HS, Park MS, Kim JT, Kim JH, Cho KA, et al. Regulation of caveolin-1 expression determines early brain edema after experimental focal cerebral ischemia. Stroke. 2016;47(5):1336–43. https://doi.org/10.1161/STROKEAHA.116.013205.
81. Kim GW, Lewén A, Copin J, Watson BD, Chan PH. The cytosolic antioxidant, copper/zinc superoxide dismutase, attenuates blood-brain barrier disruption and oxidative cellular injury after photothrombotic cortical ischemia in mice. Neuroscience. 2001;105(4):1007–18. https://doi.org/10.1016/S0306-4522(01)00237-8.
82. Caine S, Hackett MJ, Hou H, Kumar S, Maley J, Ivanishvili Z, et al. A novel multi-modal platform to image molecular and elemental alterations in ischemic stroke. Neurobiol Dis. 2016;91:132–42. https://doi.org/10.1016/j.nbd.2016.03.006.
83. Tuor UI, Deng Q, Rushforth D, Foniok T, Qiao M. Model of minor stroke with mild peri-infarct ischemic injury. J Neurosci Methods. 2016;268:56–65. https://doi.org/10.1016/j.jneumeth.2016.04.025.
84. Nahirney PC, Reeson P, Brown CE. Ultrastructural analysis of blood-brain barrier breakdown in the peri-infarct zone in young adult and aged mice. J Cereb Blood Flow Metab. 2016;36(2):413–25. https://doi.org/10.1177/0271678X15608396.
85. Lapilover EG, Lippmann K, Salar S, Maslarova A, Dreier JP, Heinemann U, et al. Peri-infarct blood-brain barrier dysfunction facilitates induction of spreading depolarization associated with epileptiform discharges. Neurobiol Dis. 2012;48(3):495–506. https://doi.org/10.1016/j.nbd.2012.06.024.
86. Wester P, Watson BD, Prado R, Dietrich WD. A photothrombotic 'ring' model of rat stroke-in-evolution displaying putative

penumbral inversion. Stroke. 1995;26(3):444–50. https://doi.org/10.1161/01.STR.26.3.444.
87. Gu WG, Brännström T, Jiang W, Wester P. A photothrombotic ring stroke model in rats with remarkable morphological tissue recovery in the region at risk. Exp Brain Res. 1999;125:171–83.
88. Hilger T, Blunk JA, Hoehn M, Mies G, Wester P. Characterization of a novel chronic photothrombotic ring stroke model in rats by magnetic resonance imaging, biochemical imaging, and histology. J Cereb Blood Flow Metab. 2004;24(7):789–97. https://doi.org/10.1097/01.WCB.0000123905.17746.DB.
89. Nakamura K, Kamouchi M, Arimura K, Nishimura A, Kuroda J, Ishitsuka K, et al. Extracellular acidification activates cAMP responsive element binding protein via Na+/H+ exchanger isoform 1-mediated Ca^{2+}oscillation in central nervous system pericytes. Arterioscler Thromb Vasc Biol. 2012;32(11):2670–7. https://doi.org/10.1161/ATVBAHA.112.254946.
90. Yao H, Takasawa R, Fukuda K, Shiokawa D, Sadanaga-Akiyoshi F, Ibayashi S, et al. DNA fragmentation in ischemic core and penumbra in focal cerebral ischemia in rats. Brain Res Mol Brain Res. 2001;91(1-2):112–8. https://doi.org/10.1016/S0169-328X(01)00135-8.
91. Eichenbaum JW, Pevsner PH, Pivawer G, Kleinman GM, Chiriboga L, Stern A, et al. A murine photochemical stroke model with histologic correlates of apoptotic and nonapoptotic mechanisms. J Pharmacol Toxicol Methods. 2002;47(2):67–71. https://doi.org/10.1016/S1056-8719(02)00215-0.
92. Hu X, Johansson IM, Brännström T, Olsson T, Wester P. Long-lasting neuronal apoptotic cell death in regions with severe ischemia after photothrombotic ring stroke in rats. Acta Neuropathol. 2002;104(5):462–70. https://doi.org/10.1007/s00401-002-0579-8.
93. Gu W, Brännström T, Wester P. Cortical neurogenesis in adult rats after reversible photothrombotic stroke. J Cereb Blood Flow Metab. 2000;20(8):1166–73. https://doi.org/10.1097/00004647-200008000-00002.
94. Kharlamov A, Uz T, Joo JY, Manev H. Pharmacological characterization of apoptotic cell death in a model of photothrombotic brain injury in rats. Brain Res. 1996;734:1–9.
95. Love S. Apoptosis and brain ischaemia. Prog Neuro-Psychopharmacol Biol Psychiatry. 2003;27(2):267–82. https://doi.org/10.1016/S0278-5846(03)00022-8.
96. Van Hoecke M, Prigent-Tessier AS, Garnier PE, Bertrand NM, Filomenko R, Bettaieb A, et al. Evidence of HIF-1 functional binding activity to caspase-3 promoter after photothrombotic cerebral ischemia. Mol Cell Neurosci. 2007;34(1):40–7. https://doi.org/10.1016/j.mcn.2006.09.009.
97. Chen TY, Lee MY, Chen HY, Kuo YL, Lin SC, Wu TS, et al. Melatonin attenuates the postischemic increase in blood-brain barrier permeability and decreases hemorrhagic transformation of tissue-plasminogen activator therapy following ischemic stroke in mice. J Pineal Res. 2006;40(3):242–50. https://doi.org/10.1111/j.1600-079X.2005.00307.x.
98. Bierbower SM, Choveau FS, Lechleiter JD, Shapiro MS. Augmentation of M-type (KCNQ) potassium channels as a novel strategy to reduce stroke-induced brain injury. J Neurosci. 2015;35(5):2101–11. https://doi.org/10.1523/JNEUROSCI.3805-14.2015.
99. Piao MS, Lee JK, Jang JW, Hur H, Lee SS, Xiao L, et al. Melatonin improves functional outcome via inhibition of matrix metalloproteinases-9 after photothrombotic spinal cord injury in rats. Acta Neurochir. 2014;156(11):2173–82. https://doi.org/10.1007/s00701-014-2119-4.
100. Aerden LA, Kessels FA, Rutten BP, Lodder J, Steinbusch HW. Diazepam reduces brain lesion size in a photothrombotic model of focal ischemia in rats. Neurosci Lett. 2004;367(1):76–8. https://doi.org/10.1016/j.neulet.2004.05.083.
101. Liu Y, Sun Q, Chen X, Jing L, Wang W, Yu Z, et al. Linolenic acid provides multi-cellular protective effects after photothrombotic cerebral ischemia in rats. Neurochem Res. 2014;39(9):1797–808. https://doi.org/10.1007/s11064-014-1390-3.
102. Demougeot C, Van Hoecke M, Bertrand N, Prigent-Tessier A, Mossiat C, Beley A, et al. Cytoprotective efficacy and mechanisms of the liposoluble iron chelator 2,2′-dipyridyl in the rat photothrombotic ischemic stroke model. J Pharmacol Exp Ther. 2004;311(3):1080–7. https://doi.org/10.1124/jpet.104.072744.
103. Van Hoecke M, Prigent-Tessier A, Bertrand N, Prevotat L, Marie C, Beley A. Apoptotic cell death progression after photothrombotic focal cerebral ischaemia: effects of the lipophilic iron chelator 2,2′-dipyridyl. Eur J Neurosci. 2005;22(5):1045–56. https://doi.org/10.1111/j.1460-9568.2005.04297.x.
104. Millerot-Serrurot EL, Bertrand N, Mossiat C, Faure P, Prigent-Tessier A, Garnier P, et al. Temporal changes in free iron levels after brain ischemia relevance to the timing of iron chelation therapy in stroke. Neurochem Int. 2008;52(8):1442. https://doi.org/10.1016/j.neuint.2008.04.002.
105. López-Valdés HE, Clarkson AN, Ao Y, Charles AC, Carmichael ST, Sofroniew MV, et al. Memantine enhances recovery from stroke. Stroke. 2014;45(7):2093–100. https://doi.org/10.1161/STROKEAHA.113.004476.
106. Jang JY, Choi YW, Kim HN, Kim YR, Hong JW, Bae DW, et al. Neuroprotective effects of a novel single compound 1-methoxyoctadecan-1-ol isolated from *Uncaria sinensis* in primary cortical neurons and a photothrombotic ischemia model. PLoS One. 2014;9:e85322. https://doi.org/10.1371/journal.pone.0085322. eCollection 2014
107. Lorrio S, Gómez-Rangel V, Negredo P, Egea J, Leon R, Romero A, et al. Novel multitarget ligand ITH33/IQM9.21 provides neuroprotection in in vitro and in vivo models related to brain ischemia. Neuropharmacology. 2013;67:403–11. https://doi.org/10.1016/j.neuropharm.2012.12.001.
108. Zou LY, Cheung RT, Liu S, Li G, Huang L. Melatonin reduces infarction volume in a photothrombotic stroke model in the wild-type but not cyclooxygenase-1-gene knockout mice. J Pineal Res. 2006;41(2):150–6. https://doi.org/10.1111/j.1600-079X.2006.00349.x.
109. Parada E, Buendia I, León R, Negredo P, Romero A, Cuadrado A, et al. Neuroprotective effect of melatonin against ischemia is partially mediated by alpha-7 nicotinic receptor modulation and HO-1 overexpression. J Pineal Res. 2014;56(2):204–12. https://doi.org/10.1111/jpi.12113.
110. Jang JW, Lee JK, Lee MC, Piao MS, Kim SH, Kim HS. Melatonin reduced the elevated matrix metalloproteinase-9 level in a rat photothrombotic stroke model. J Neurol Sci. 2012;323(1–2):221–7. https://doi.org/10.1016/j.jns.2012.09.021.
111. Jang JW, Lee JK, Hur H, Kim TW, Joo SP, Piao MS. Rutin improves functional outcome via reducing the elevated matrix metalloproteinase-9 level in a photothrombotic focal ischemic model of rats. J Neurol Sci. 2014;339(1–2):75–80. https://doi.org/10.1016/j.jns.2014.01.024.
112. Park CH, Shin TK, Lee HY, Kim SJ, Lee WS. Matrix metalloproteinase inhibitors attenuate neuroinflammation following focal cerebral ischemia in mice. Korean J Physiol Pharmacol. 2011;15(2):115–22. https://doi.org/10.4196/kjpp.2011.15.2.115.
113. Parada E, Egea J, Buendia I, Negredo P, Cunha AC, Cardoso S, et al. The microglial α7-acetylcholine nicotinic receptor is a key element in promoting neuroprotection by inducing heme oxygenase-1 via nuclear factor erythroid-2-related factor 2. Antioxid Redox Signal. 2013;19(11):1135–48. https://doi.org/10.1089/ars.2012.4671.
114. Porritt MJ, Andersson HC, Hou L, Nilsson Å, Pekna M, Pekny M, et al. Photothrombosis-induced infarction of the mouse cerebral cortex is not affected by the Nrf2-activator sulforaphane. PLoS

One. 2012;7(7):e41090. https://doi.org/10.1371/journal.pone.0041090.

115. Madinier A, Bertrand N, Rodier M, Quirié A, Mossiat C, Prigent-Tessier A. Ipsilateral versus contralateral spontaneous post-stroke neuroplastic changes: involvement of BDNF? Neuroscience. 2013;231:169–81. https://doi.org/10.1016/j.neuroscience.2012.11.054.
116. Schäbitz WR, Berger C, Kollmar R, Seitz M, Tanay E, Kiessling M, et al. Effect of brain-derived neurotrophic factor treatment and forced arm use on functional motor recovery after small cortical ischemia. Stroke. 2004;35(4):992–7. https://doi.org/10.1161/01.STR.0000119754.85848.0D.
117. Li PC, Jiao Y, Ding J, Chen YC, Cui Y, Qian C, et al. Cystamine improves functional recovery via axon remodeling and neuroprotection after stroke in mice. CNS Neurosci Ther. 2015;21(3):231–40. https://doi.org/10.1111/cns.12343.
118. Zhan H, Sun SJ, Cai J, Li YQ, CL H, Lee DH, et al. The effect of an NgR1 antagonist on the neuroprotection of cortical axons after cortical infarction in rats. Neurochem Res. 2013;38(7):1333–40. https://doi.org/10.1007/s11064-013-1026-z.
119. Shin TK, Kang MS, Lee HY, Seo MS, Kim SG, Kim CD, et al. Fluoxetine and sertraline attenuate postischemic brain injury in mice. Korean J Physiol Pharmacol. 2009;13(3):257–63. https://doi.org/10.4196/kjpp.2009.13.3.257.
120. Romanova GA, Shakova FM, Barskov IV, Stel'mashuk EV, Genrikhs EE, Cheremnykh AM, et al. Neuroprotective and antiamnesic effect of erythropoietin derivatives after experimental ischemic injury of cerebral cortex. Bull Exp Biol Med. 2015;158(3):318–21. https://doi.org/10.1007/s10517-015-2751-x.
121. Urnukhsaikhan E, Mishig-Ochir T, Kim SC, Park JK, Seo YK. Neuroprotective effect of low frequency-pulsed electromagnetic fields in ischemic stroke. Appl Biochem Biotechnol. 2017;181(4):1360–71. https://doi.org/10.1007/s12010-016-2289-z.
122. Sutherland BA, Minnerup J, Balami JS, Arba F, Buchan AM, Kleinschnitz C. Neuroprotection for ischaemic stroke: translation from the bench to the bedside. Int J Stroke. 2012;7(5):407–18. https://doi.org/10.1111/j.1747-4949.2012.00770.x.